Computer Methods and Programs in Biomedicine 171 (2019) 133–140

Contents lists available at ScienceDirect

Computer Methods and Programs in Biomedicine

journal homepage: www.elsevier.com/locate/cmpb

Model individualization for artificial pancreas ☆

Mirko Messori[a,*], Chiara Toffanin[a], Simone Del Favero[b], Giuseppe De Nicolao[c], Claudio Cobelli[b], Lalo Magni[a]

[a] Department of Civil Engineering and Architecture, University of Pavia, Pavia, Italy
[b] Department of Information Engineering, University of Padova, Padova, Italy
[c] Department of Industrial and Information Engineering, University of Pavia, Pavia, Italy

ARTICLE INFO

Article history:
Received 18 December 2015
Revised 13 May 2016
Accepted 28 June 2016

Keywords:
Constrained optimization
Nonparametric identification
Model predictive control
Linear systems
Type 1 diabetes

ABSTRACT

Background and Objective: The inter-subject variability characterizing the patients affected by type 1 diabetes mellitus makes automatic blood glucose control very challenging. Different patients have different insulin responses, and a control law based on a non-individualized model could be ineffective. The definition of an individualized control law in the context of artificial pancreas is currently an open research topic. In this work we consider two novel identification approaches that can be used for individualizing linear glucose–insulin models to a specific patient.

Methods: The first approach belongs to the class of black-box identification and is based on a novel kernel-based nonparametric approach, whereas the second is a gray-box identification technique which relies on a constrained optimization and requires to postulate a model structure as prior knowledge. The latter is derived from the linearization of the average nonlinear adult virtual patient of the UVA/Padova simulator. Model identification and validation are based on in silico data collected during simulations of clinical protocols designed to produce a sufficient signal excitation without compromising patient safety. The identified models are evaluated in terms of prediction performance by means of the coefficient of determination, fit, positive and negative max errors, and root mean square error.

Results: Both identification approaches were used to identify a linear individualized glucose–insulin model for each adult virtual patient of the UVA/Padova simulator. The resulting model simulation performance is significantly improved with respect to the performance achieved by a linear average model.

Conclusions: The approaches proposed in this work have shown a good potential to identify glucose–insulin models for designing individualized control laws for artificial pancreas.

1. Introduction

Type 1 Diabetes Mellitus (T1DM), also known as *insulin-dependent* or *juvenile* diabetes, is a metabolic disorder characterized by chronic hyperglycemia that occurs when the pancreas is no longer able to produce insulin. Patients affected by T1DM are dependent on exogenous insulin administration to maintain the Blood Glucose (BG) concentration (also called *glycemia*) within the so called *euglycemic* range, which spans from 70 mg/dl to 180 mg/dl. Manual insulin administration is complex since there is the need to estimate the insulin dose to inject subcutaneously both during mealtimes and fasting periods. If the injected insulin is underestimated, the patient can experience *hyperglycemia*, which is generally associated to BG levels higher than 180–200 mg/dl. In addition, symptoms may not start to become noticeable until even higher BG levels, such as 250–300 mg/dl. Chronic hyperglycemia can produce a wide variety of serious complications over a period of years, including damages to kidneys, nervous system, cardiovascular system, retina, feet/legs and nerves (i.e. diabetic neuropathy). On the other hand, if the injected insulin is overestimated, the patient can experience *hypoglycemia*, which is associated to a BG level lower than 70 mg/dl. Hypoglycemia can cause tachycardia, shakiness, strong headache, sudden mood changes, hunger, sweating, dizziness and nausea, and, if severe, can lead to seizures, loss of consciousness, coma, or death.

The Artificial Pancreas (AP) is a system thought to automate the exogenous insulin supply and is composed of a subcutaneous glucose sensor, which allows Continuous Glucose Monitoring (CGM), a

☆ This paper is submitted to a Special Issue of Computer Methods and Programs in Biomedicine following the **IFAC BMS 2015** meeting in Berlin.

* Corresponding author. Identification and Control of Dynamic Systems Laboratory (ICDL), 5, A. Ferrata Street, 27100 Pavia, Italy. Fax: +39 0382 985589.
E-mail address: mirko.messori01@ateneopv.it (M. Messori).

https://doi.org/10.1016/j.cmpb.2016.06.006
0169-2607/

subcutaneous insulin pump, and a control algorithm. Recently, several research projects on AP were supported by the Juvenile Diabetes Research Foundation, the European Commission, and the National Institutes of Health (see Refs. [1–9]). The core of the AP is the control algorithm, which is in charge of continually estimating the quantity of insulin to inject in the subcutaneous tissue on the basis of the subcutaneous continuous glucose measurements. A detailed description of the state of the art of the considered AP system can be found in Ref. [10], where the adopted control algorithm is a Model Predictive Control (MPC). MPC synthesizes a controller on the basis of a model that describes the dynamics of the process under control (i.e. the biological dynamics of the patient). A complex metabolic model was first introduced in Ref. [11] and then improved in Ref. [12]. This model is highly nonlinear and time-varying and its implementation in a MPC law is computationally demanding. However, as shown in Refs. [13,14], a linear time-invariant approximation of glucose–insulin interaction is adequate to capture the essential dynamics to design an effective and safe MPC, while guaranteeing reduced complexity and low computational burden in the MPC implementation. This fact was also confirmed by several clinical trials performed in silico [14–20] and in vivo [7,9,21–27] through MPC synthesized on the basis of a linear model.

Diabetic patients are characterized by a substantial inter-subject variability that may limit the closed-loop control performance achievable by a non-individualized controller. Thus, a significant step forward would be represented by the controller individualization that, however, is very challenging. The control performance could be limited even by the patient intra-subject variability, which would require a recursively adaptive control law [28]. Different approaches can be considered like multivariable adaptive control [29,30] or run-to-run strategies used for daily adaptation of basal insulin [31], insulin boluses [32–35], or MPC cost function [36].

In order to synthesize an individualized MPC, a patient-tailored glucose–insulin model is needed. The Nonparametric (NP) approach for linear models identification presented in Ref. [37] was applied to simulated data. An in silico trial was also performed, demonstrating that the MPC synthesized on the basis of the individualized models significantly improves closed-loop control performance. In addition to the NP approach, a parametric identification technique driven by Constrained Optimization (CO) is presented, where the identified models are characterized by a fixed structure that is postulated as prior knowledge. Models identification and test are based on in silico data collected during closed-loop simulations of clinical protocols designed to produce a sufficient input–output excitation without compromising the patient safety. The identified models are evaluated in terms of prediction performance by means of the Coefficient of Determination (COD), FIT, Positive and Negative Max Errors (PME and NME, respectively), and Root Mean Square Error (RMSE). The resulting performance is compared with the performance achieved by the NP models presented in Ref. [37] and with the average linear model used to synthesize the linear MPC introduced in Ref. [19], which was also used in several clinical experiments.

2. Methods

Given the large inter-subject variability, a significant improvement of blood-glucose control is expected using a control law individualized on patient-specific glucose–insulin responses instead of resorting to an average model [14,19]. Two methods devoted to the patient glucose–insulin dynamics identification are presented in this section. Both the identification approaches are used to identify 100 linear models representing the dynamics of the 100 virtual patients of the adult population of the UVA/Padova simulator [12]. Identification (including parameter estimation and, if needed, model validation) and model test are based on input–output data achieved in closed-loop simulations performed through the MPC presented in Ref. [19].

2.1. Nonparametric identification

The NP approach belongs to the class of black-box identification and is used to identify the glucose–insulin dynamics of the patient from measured input–output data. As shown in Ref. [37], the identified model can be used to synthesize a patient-tailored MPC, substantially increasing the closed-loop control performance. This approach relies on a kernel-based regression and is exploited to identify a one-step ahead predictor that is subsequently converted in a state space model obtained through a minimal realization of a given dimension. The final aim is to obtain a linear dynamical model of the form

$$y(t) = \sum_{k=1}^{\infty} q_u(k)u(t-k) + \sum_{k=1}^{\infty} q_d(k)d(t-k) + \sum_{k=0}^{\infty} w(k)e(t-k) \tag{1}$$

where u and d are the model inputs and represent the differential subcutaneous infused insulin with respect to the patient basal insulin and the ingested carbohydrates (CHO), respectively; y is the model output and represents the differential subcutaneous glucose concentration with respect to the basal glucose G_b; and e is a white Gaussian noise signal representing the uncertainties affecting the model.

2.1.1. Linear predictor estimation

In order to better illustrate this method, let us consider the following linear one-step ahead predictor:

$$\hat{y}(t) = \sum_{k=1}^{\infty} f(k)y(t-k) + \sum_{k=1}^{\infty} g_1(k)u(t-k) + \sum_{k=1}^{\infty} g_2(k)d(t-k) \tag{2}$$

where $\hat{y}$ is the predicted output (i.e. predicted differential subcutaneous glucose concentration), f is the output discrete impulse response, and g_1 and g_2 are the input discrete impulse responses, respectively (i.e. impulse responses associated to insulin and meal inputs), which have to be estimated from noisy measurements. The estimation of the unknown impulse responses can be performed by solving an optimization problem in an infinite-dimensional functional space given by a Reproducing Kernel Hilbert Space (RKHS). The chosen kernel should reflect the properties of the functions to be estimated and its choice is a key point in the NP approaches. In this case, the chosen kernel K is the Stable Spline Kernel (SSK) proposed in Ref. [38], where the generic impulse response f_{SSK} to identify is seen as a realization of a zero-mean Gaussian random process whose covariance can be written as

$$\begin{aligned} Cov(f_{SSK}(k), f_{SSK}(l)) &= \lambda^2 K(k,l) \\ &= \lambda^2 \left(\frac{e^{-\tau(k+l)} e^{-\tau \max(k,l)}}{2} - \frac{e^{-3\tau \max(k,l)}}{6} \right) \end{aligned} \tag{3}$$

with $k, l = 1, 2, \ldots, \infty$, $\tau > 0$, and $\lambda > 0$. As explained in Ref. [38], SSK includes a prior which preserves exponentials with rate constant τ, which is a good characteristic in the context of linear dynamic systems identification. Moreover, the stability of the identified impulse response is guaranteed, and a linear bounded-input bounded-output stable system can be identified from noisy measurements without postulating a parametric structure. Following the methodology introduced in Ref. [39], by defining K_f, K_{g1} and K_{g2} as the SSK of f, g_1 and g_2 of (2), respectively, and letting $\mathscr{H}_f$,

$\mathscr{H}_{g1}$ and $\mathscr{H}_{g2}$ denote the RKHS of deterministic functions on $\mathbb{N}$ associated with K_f, K_{g1} and K_{g2} (with norms denoted by $\|\cdot\|_{\mathscr{H}_f}$, $\|\cdot\|_{\mathscr{H}_{g1}}$, and $\|\cdot\|_{\mathscr{H}_{g2}}$), the stable spline estimators $\hat{f}$, $\hat{g}_1$ and $\hat{g}_2$ of f, g_1 and g_2 are obtained from the solution of the following Tikhonov-type variational problem:

$$\left(\hat{f},\hat{g}_1,\hat{g}_2\right) = \arg \min_{h_f\in\mathscr{H}_f, h_{g1}\in\mathscr{H}_{g1}, h_{g2}\in\mathscr{H}_{g2}} \left\{ \left\|y^+ - \tilde{A}h_f - \tilde{B}h_{g1} - \tilde{C}h_{g2}\right\|^2 + \gamma_f \|h_f\|^2_{\mathscr{H}_f} + \gamma_{g1}\|h_{g1}\|^2_{\mathscr{H}_{g1}} + \gamma_{g2}\|h_{g2}\|^2_{\mathscr{H}_{g2}} \right\} \quad (4)$$

with

$$\left[\tilde{A}\right]_{ji} = y(j-i), \left[\tilde{B}\right]_{ji} = u(j-i), \left[\tilde{C}\right]_{ji} = d(j-i)$$
$$i = 1,2,\ldots,\infty, j = 1,2,\ldots,n^+$$
$$y^+ = [y_1 y_2 \cdots y_{n^+}]^T$$

and where $\|\cdot\|$ is the Euclidean norm, $\gamma_f = \sigma_e^2/\lambda_f^2$, $\gamma_{g1} = \sigma_e^2/\lambda_{g1}^2$, $\gamma_{g2} = \sigma_e^2/\lambda_{g2}^2$, and n^+ is the number of future samples to consider during the identification process. In view of (3), the covariances of the impulse responses f, g_1 and g_2 include the parameters τ_f, τ_{g1}, and τ_{g2}, respectively. Here τ_f, τ_{g1}, τ_{g2}, λ_f, λ_{g1}, λ_{g2}, and σ_e are *hyperparameters* that have to be properly tuned prior to the solution of the Tikhonov problem (4). By assuming known hyperparameters, the solution of (4) is given by

$$\begin{aligned}
\hat{f} &= \lambda_f^2 K_f \tilde{A}^T \phi \\
\hat{g}_1 &= \lambda_{g1}^2 K_{g1} \tilde{B}^T \phi \\
\hat{g}_2 &= \lambda_{g2}^2 K_{g2} \tilde{C}^T \phi \\
\phi &= \left(\lambda_f^2 \tilde{A} K_f \tilde{A}^T + \lambda_{g1}^2 \tilde{B} K_{g1} \tilde{B}^T + \lambda_{g2}^2 \tilde{C} K_{g2} \tilde{C}^T + \sigma_e^2 I_{n^+}\right)^{-1} y^+
\end{aligned} \quad (5)$$

where I_{n^+} is the $n^+ \times n^+$ identity matrix.

2.1.2. Hyperparameters estimation

The solution (5) depends on the values of the hyperparameters, which have to be properly estimated. As shown in Ref. [39], by letting Υ denote the hyperparameters vector, the maximum (marginal) likelihood estimate $\hat{\Upsilon}$ of Υ is given by

$$\hat{\Upsilon} = \arg\min_{\Upsilon} J\left(y^+, \Upsilon\right)$$

with

$$J\left(y^+,\Upsilon\right) = \frac{1}{2}\ln\left(\det\left[2\pi V\left[y^+\right]\right]\right) + \frac{1}{2}\left(y^+\right)^T \left(V\left[y^+\right]\right)^{-1} y^+$$
$$V\left[y^+\right] = \lambda_f^2 \tilde{A} K_f \tilde{A}^T + \lambda_{g1}^2 \tilde{B} K_{g1} \tilde{B}^T + \lambda_{g2}^2 \tilde{C} K_{g2} \tilde{C}^T + \sigma_e^2 I_{n^+}$$

where J is the opposite log-marginal likelihood of y^+. Thus, the hyperparameters are estimated through a marginal likelihood optimization in a low-dimensional space, limiting the computational efforts needed to perform the optimization process. After their estimation, the hyperparameters are set into (4), and the minimum variance estimates (5) of the impulse responses are then obtained.

2.1.3. Individualized linear model

The one-step ahead predictor (2) must be converted in a linear model usable for synthesizing an individualized MPC. Given the predicted output $\hat{y}(t)$ it holds that

$$y(t) = \hat{y}(t) + e(t)$$

where $e(t)$ is a white Gaussian noise signal affecting the reliability of the predictions $\hat{y}(t)$ and whose variance is estimated through the hyperparameter σ_e^2. Thus, the input–output form of the model (1) can be approximated as follows:

$$y(t) = \frac{\sum_{k=1}^{p_l} g_1(k) z^{-k}}{1 - \sum_{k=1}^{p_l} f(k) z^{-k}} u(t) + \frac{\sum_{k=1}^{p_l} g_2(k) z^{-k}}{1 - \sum_{k=1}^{p_l} f(k) z^{-k}} d(t) + \frac{1}{1 - \sum_{k=1}^{p_l} f(k) z^{-k}} e(t)$$

where the Z-transform formalism has been used. The approximation consists in truncating the summations to p_l, a tunable parameter that however can be arbitrarily large. The Z-transforms of q_u, q_d and w of (1) are given by

$$Q_u(z) = \frac{\sum_{k=1}^{p_l} g_1(k) z^{-k}}{1 - \sum_{k=1}^{p_l} f(k) z^{-k}}, \quad Q_d(z) = \frac{\sum_{k=1}^{p_l} g_2(k) z^{-k}}{1 - \sum_{k=1}^{p_l} f(k) z^{-k}},$$
$$W(z) = \frac{1}{1 - \sum_{k=1}^{p_l} f(k) z^{-k}}$$

and admit a minimal realization of dimension p_l. It is worth to emphasize that the matrices $\tilde{A}$, $\tilde{B}$ and $\tilde{C}$ of (4) are theoretically infinite-dimensional, but, in practice, their dimensions are truncated according to the chosen predictor length p_l. Since the impulse responses f, g_1 and g_2 are not known, they are substituted with the identified impulse responses $\hat{f}$, $\hat{g}_1$ and $\hat{g}_2$ coming from (5), thus resulting in the definition of the following identified Z-transforms:

$$\hat{Q}_u(z) = \frac{\sum_{k=1}^{p_l} \hat{g}_1(k) z^{-k}}{1 - \sum_{k=1}^{p_l} \hat{f}(k) z^{-k}}, \quad \hat{Q}_d(z) = \frac{\sum_{k=1}^{p_l} \hat{g}_2(k) z^{-k}}{1 - \sum_{k=1}^{p_l} \hat{f}(k) z^{-k}},$$
$$\hat{W}(z) = \frac{1}{1 - \sum_{k=1}^{p_l} \hat{f}(k) z^{-k}}$$

Given the identified Z-transforms, the following model can be defined:

$$y(k) = \hat{Q}_u(z)u(k) + \hat{Q}_d(z)d(k) + \hat{W}(z)e(k) \quad (6)$$

where a mixed Z/discrete-time representation has been used. Hence, the minimal state space realization can be written as follows:

$$\begin{cases} x_{NP}(k+1) = A_{NP}x_{NP}(k) + B_{NP}u(k) + M_{NP}d(k) + W_{NP_x}e(k) \\ y(k) = C_{NP}x_{NP}(k) + W_{NP_y}e(k) \end{cases}$$

where x_{NP} is a vector of maximum dimension p_l containing the internal states of the identified NP model, and A_{NP}, B_{NP}, C_{NP}, M_{NP} are matrices of proper dimensions describing the system dynamics. The relationship between the white Gaussian noise e and the identified model is described through the column vector W_{NP_x} (having the same number of elements of x_{NP}) and the scalar value W_{NP_y}. This is the definition of an augmented model that, in addition to the system dynamics, defines also an estimation of the model uncertainties driven by a zero-mean white Gaussian noise e with estimated variance σ_e^2.

2.2. Identification through constrained optimization

Unlike the NP case, this approach is a gray-box identification and requires to postulate a parametric structure of the model to identify. The postulated parametric structure is obtained starting from the linearization of the UVA/Padova metabolic model [12] around a basal working point representing the steady state of the patient during fasting periods [18,19], and is defined as follows:

$$\begin{cases} x_{CO}(k+1) = A_{CO}x_{CO}(k) + B_{CO}u(k) + M_{CO}d(k) \\ y(k) = C_{CO}x_{CO}(k) \end{cases} \tag{7}$$

where $x_{CO}(k)$ and $y(k)$ are the internal states and the model output (i.e. the differential subcutaneous glucose concentration with respect to the basal glucose G_b), and $u(k)$ and $d(k)$ are the two inputs representing the differential insulin infusion with respect to the basal insulin and the CHO intake, respectively. The above matrices, to be identified, have dimensions $A_{CO} \in \mathbb{R}^{n\times n}$, $B_{CO} \in \mathbb{R}^{n\times 1}$, $C_{CO} \in \mathbb{R}^{1\times n}$, $M_{CO} \in \mathbb{R}^{n\times 1}$, with n the number of internal states of the linearization of the model in Ref. [12]. Several elements have been fixed equal to zero according to the structure of the linearization of the UVA/Padova metabolic model, in this way including the a-priori information on the model and also reducing the computational burden of the optimization.

2.2.1. Optimization problem definition

The non-zero elements of the matrices are parameters of the following CO problem:

$$\begin{aligned} &\left(A^o_{CO}, B^o_{CO}, C^o_{CO}, M^o_{CO}\right) \\ &= \arg \min_{A_{CO},B_{CO},C_{CO},M_{CO}} J_{CO}(A_{CO}, B_{CO}, C_{CO}, M_{CO}, U, D, Y_{MA}, x_{CO}(0)) \end{aligned} \tag{8}$$

such that

$$\begin{aligned} &A^{\min}_{CO} \le A_{CO} \le A^{\max}_{CO} \\ &B^{\min}_{CO} \le B_{CO} \le B^{\max}_{CO} \\ &C^{\min}_{CO} \le C_{CO} \le C^{\max}_{CO} \\ &M^{\min}_{CO} \le M_{CO} \le M^{\max}_{CO} \\ &|\lambda_l(A_{CO})| < 1, l = 1, 2, \ldots, n \end{aligned} \tag{9}$$

$$\frac{\sum_{k=0}^{p_{lCO}} \max\{g_{1CO}(k), 0\}}{\sum_{k=0}^{p_{lCO}} -\min\{g_{1CO}(k), 0\}} < k^{\%}_p \tag{10}$$

$$-\sum_{k=0}^{p_{lCO}} g_{1CO}(k) > k^{ss}_p \cdot \sum_{k=0}^{p_{lCO}} g_{2CO}(k) \tag{11}$$

$$\sum_{k=0}^{p_{lCO}} g_{1CO}(k) < 0, \quad \sum_{k=0}^{p_{lCO}} g_{2CO}(k) > 0 \tag{12}$$

where g_{1CO} and g_{2CO} are the insulin and meal impulse responses derived by the identified CO model, respectively; p_{lCO} represents their maximum length; $k^{\%}_p > 0$ is a threshold which denotes the maximum allowed inverse excursion in the insulin impulse response; $k^{ss}_p > 0$ is a factor which relates the steady state gains of insulin and meal impulse responses; and $\lambda_l(A_{CO})$ denotes the l-th eigenvalue of the A_{CO} matrix, thus defining a stability constraint.

The cost J_{CO} is defined as follows:

$$\begin{aligned} &J_{CO}(A_{CO}, B_{CO}, C_{CO}, M_{CO}, U, D, Y_{MA}, x_{CO}(0)) \\ &= \underbrace{\left\| \sum_{j=0}^{N_{CO}} [C_{CO}x_{CO}(j) - y_{MA}(j) + G_b] \right\|^2}_{\text{Squared residuals}} \\ &+ \underbrace{\sum_{j=1}^{n} |\min\left\{\min\left(X_{CO_j}\right) - \delta^{\min}_j, 0\right\}|^{p_s}}_{\text{Lower states soft constraints}} \\ &+ \underbrace{\sum_{j=1}^{n} |\max\left\{\max\left(X_{CO_j}\right) - \delta^{\max}_j, 0\right\}|^{p_s}}_{\text{Upper states soft constraints}} \end{aligned} \tag{13}$$

where $x_{CO}(j)$ contains the model state at time j, and $p_s > 1$ is the power of the terms associated to the lower and upper state soft constraints. The cost J_{CO} depends on the input–output data coming from the considered identification scenario. Indeed, the vectors U and D represent the inputs (infused insulin and ingested meals, respectively) and are defined as

$$\begin{aligned} U &= \begin{bmatrix} u(0) & u(1) & \cdots & u(N_{CO}-1) \end{bmatrix} \\ D &= \begin{bmatrix} d(0) & d(1) & \cdots & d(N_{CO}-1) \end{bmatrix} \end{aligned}$$

with N_{CO} representing the number of considered samples, whereas the vector Y_{MA} represents the output (CGM sensor measurements) and is defined as

$$Y_{MA} = \begin{bmatrix} y_{MA}(0) & y_{MA}(1) & \cdots & y_{MA}(N_{CO}) \end{bmatrix}$$

Each output measurement is "filtered" by the following Moving Average (MA):

$$y_{MA}(k) = \frac{\sum_{j=0}^{N_{MA}-1} CGM(k-j)}{N_{MA}} \tag{14}$$

where N_{MA} is the chosen MA length. The first addend of the cost (13) accounts for the model fit to the data and depends on the unknown matrix entries to be estimated and also on the initial state guess $x_{CO}(0)$. The second and the third addends of the cost (13) define lower and upper state soft constraints, respectively, which depend on the following predicted state trajectories X_{CO_j}:

$$X_{CO_j} = \begin{bmatrix} x_{CO_j}(0) & x_{CO_j}(1) & \cdots & x_{CO_j}(N_{CO}) \end{bmatrix}$$

with j denoting the jth model state. This means that the cost is forced to substantially increase if the minimum or the maximum value of each state trajectory exceeds at any time the imposed limits $\delta^{\min}_j < 0$ and $\delta^{\max}_j > 0$, respectively. The introduction of the state soft constraints proved to be useful in preventing the convergence of the optimizer to local minima that would result in the identification of systems with poor prediction capabilities or, even worse, that would be non-stable (as discussed in section 2.2.2).

2.2.2. Solution

The CO problem (8) must be properly initialized with an initial guess of the unknown matrices and of the state $x_{CO}(0)$. Indeed, the computational time needed to find a reliable solution may be significantly affected by the chosen initialization values. In order to automate the initial guess determination, a simulated annealing approach [40] has been exploited. The simulated annealing process is initialized by considering the model matrices of the linearized average adult virtual patient and its solution is then passed as initial guess in the Matlab® *fminsearch* optimizer, which is a very efficient optimizer designed for non-smooth nonlinear functions.

Table 1
Identification protocol for NP approach.

	Time (hh:MM)	Meal	CHO (g)	Duration (min)	Insulin Bolus	
Day 1	06:30	B	40	15	Bolus on time	Parameters Estimation
	09:00	S	20	15	No bolus	
	12:30	L	50	15	Bolus on time	
	15:30	S	20	15	No bolus	
	19:00	D	90	15	Bolus at 18:30	
	23:30	S	15	5	No bolus	
Day 2	07:00	B	60	15	Bolus on time	
	09:00	S	20	15	No bolus	
	12:00	L	60	15	Bolus at 11:00	
	16:20	S	20	15	No bolus	
	19:45	D	60	15	Bolus at 22:00 for 15 g	
Day 3	01:30	S	15	5	No bolus	
	07:30	B	40	15	Bolus on time	
	11:00	S	35	15	Bolus at 10:40	
	13:00	L	50	15	Bolus at 13:40 for 20 g	
	20:00	D	85	15	Bolus at 19:50	

B is Breakfast, L is Lunch, D is Dinner, and S is Snack. All data are used to identify the models parameters.

Since the fminsearch solver is not able to handle constraints, the optimization is iterated and, at the end of each iteration, the satisfaction of the constraints (9)–(12) is verified. If so, the model obtained at the current iteration is stored before initiating the subsequent iteration. Note that the lower and upper state soft constraints and the linear model dynamics are included in the optimization cost (13). Hence, these constraints are implicitly satisfied by the optimization process driven by the fminsearch solver.

In order to minimize the risk of overfitting, the achieved linear model predictions are evaluated at the end of each iteration on a validation set in terms of the COD and FIT indices defined in (15) and (16), respectively. The iterations are continued until one of the two following stopping conditions are verified.

1. Stop because of overfitting detected:
   - the cost J_{CO} is lower than a predefined threshold $t_h^{CO} > 0$
   - the current FIT and COD evaluated on a validation scenario are lower than the FIT and COD evaluated in the previous iteration
2. Stop because cost is not decreasing:
   - Condition 1 is not verified
   - the percentage of the decrease between the cost at the current iteration and the cost at the previous iteration is lower than a predefined threshold $\alpha_{\%}^{CO} \in [0 \quad 100]$

Condition 1 denotes the successful identification of the linear model. If overfitting is detected, the fminsearch iterations are stopped and the model identified at the previous iteration (i.e. before encountering overfitting) is stored. Condition 2 is introduced to avoid infinite iterations in case of impossibility to identify a valid linear model. If the iterations are stopped because of this condition, the identified model at the current iteration is stored but there are no guarantees on the model prediction performance and stability.

2.3. Simulation scenarios

The identification scenario of the NP technique is a three-day protocol (Table 1) simulated in closed-loop and composed of three meals per day (breakfast, lunch, and dinner) with additional snacks in each day controlled without meal announcement (see Ref. [18] for details on meal announcement). This scenario is used for model parameter estimation purposes.

The identification scenario of the CO technique is composed of four days. The first day includes three meals and one snack and is used for model parameter estimation (only 16 hours are considered, from 6:00 to 22:00). The remaining days are used for validation purposes (Table 2). It is worth to emphasize that there are no restrictions on the input–output data characteristics used for

Table 2
Identification protocol for CO approach.

	Time (hh:MM)	Meal	CHO (g)	Duration (min)	Insulin Bolus	
Day 1	08:00	B	60	15	Bolus on time	Parameters Estimation
	13:00	L	60	15	Bolus at 14:00	
	17:00	S	30	15	No bolus	
	20:00	D	80	15	Bolus on time	
Day 2	08:00	B	50	15	Bolus OK	Validation
	10:00	S	15	5	No bolus	
	13:00	L	35	15	Bolus OK	
	19:00	D	80	15	Bolus OK	
	22:00	S	20	15	Bolus OK	
Day 3	06:30	B	40	15	Bolus OK	
	09:30	S	20	15	No bolus	
	12:30	L	45	15	Bolus at 12:00 for 50 g	
	17:00	S	20	15	Bolus OK	
	20:00	D	70	15	Bolus at 20:30	
	23:00	S	20	15	No bolus	
Day 4	08:00	B	35	15	Bolus OK	
	11:30	S	20	15	Bolus OK	
	13:30	L	60	15	Bolus at 13:30 for 30 g	
	16:30	S	20	15	No bolus	
	20:30	D	90	15	Bolus OK	

B is Breakfast, L is Lunch, D is Dinner, and S is Snack. The first day is used to estimate the models parameters, the remaining days are used for validation.

Table 3
Test protocol for individualized models.

	Time (hh:MM)	Meal	CHO (g)	Duration (min)	Insulin Bolus	
Day 1	08:00	B	50	15	Bolus on time	Test
	13:00	L	50	15	Bolus on time	
	19:00	D	70	15	Bolus on time	
	23:00	S	20	15	Bolus on time	
Day 2	06:30	B	50	15	Bolus on time	
	09:30	S	15	15	No bolus	
	13:00	L	60	15	Bolus at 12:00 for 50 g	
	17:00	S	25	15	Bolus on time	
	20:00	D	90	15	Bolus at 20:15 for 70 g	
	23:00	S	15	15	No bolus	
Day 3	08:30	B	50	15	Bolus on time	
	11:30	S	20	15	Bolus on time	
	14:00	L	60	15	Bolus at 13:00 for 30 g	
	17:00	S	20	15	No bolus	
	20:30	D	100	15	Bolus on time	

B is Breakfast, L is Lunch, D is Dinner, and S is Snack.

validation. Both identification techniques have successfully identified 100 linear glucose–insulin models.

The identified models are tested in simulation by considering a three-day protocol in which meal amounts and times are set so as to represent a real life scenario, as shown in Table 3. This corresponds to test the model predictions over an infinite prediction horizon. Indeed, since the identified models are designed to synthesize an individualized infinite horizon MPC [19], their quality depends on their simulation capabilities. In order to completely decouple identification (meant as parameter estimation and, for the case of CO, also the validation phase) and test, the validation protocol considered for evaluating FIT and COD during the CO identification is substantially different from the testing protocol of Table 3.

2.4. Performance indices

The model predictions are evaluated through the following performance indices:

$$\mathrm{COD} = 100\left(1 - \frac{\|y(k) - I_g(k)\|^2}{\|I_g(k) - \bar{I}_g\|^2}\right) \in (-\infty \quad 100] \tag{15}$$

$$\mathrm{FIT} = 100\left(1 - \frac{\|y(k) - I_g(k)\|}{\|I_g(k) - \bar{I}_g\|}\right) \in (-\infty \quad 100] \tag{16}$$

$$\mathrm{PME} = \max\{\max(y(k) - I_g(k)), 0\} \in [0 \quad +\infty)$$

$$\mathrm{NME} = |\min\{\min(y(k) - I_g(k)), 0\}| \in [0 \quad +\infty)$$

$$\mathrm{RMSE} = \sqrt{\frac{\|y(k) - I_g(k)\|^2}{N_s}} \in [0 \quad +\infty)$$

where $I_g(k)$ is the subcutaneous glucose simulated by the nonlinear virtual patient of the UVA/Padova simulator, $\bar{I}_g$ is its average, and N_s is the total number of samples considered in the testing protocol.

3. Results

The testing results achieved by the presented individualization techniques applied to 100 adult virtual patients of the UVA/Padova simulator are shown in Table 4. In view of using the individualized models on an infinite horizon MPC [19], their quality has been evaluated in simulation. For this purpose, the NP models have been tested by considering the inputs $u(k)$ and $d(k)$ of (6) but not the past glucose values. It is evident that the identified models obtain a better prediction performance and all the differences with respect to the average model are statistically significant with $p < 0.001$. Although the best performance is achieved by the NP approach, the NP models are characterized by a non-fixed number of internal states which depend on the chosen minimal realization method, whereas the CO approach identifies models with a fixed number of states depending on the postulated parametric structure. Moreover, the CO approach requires a shorter identification protocol devoted to model parameters estimation, which would be more feasible in a real-life scenario. Indeed, the estimation of parameters requires a protocol designed to produce a sufficient signals excitation without compromising the patient safety, whereas no particular restrictions are imposed to the protocol used for models validation.

Table 4
Performance indices evaluated on the individualized models and on the linearized average model by simulating the test protocol of Table 3.

	Average	NP	CO
COD	−94.55	90.06†	80.35†
	[−339.37, 12.21]	[84.59, 93.06]	[65.45, 88.80]
FIT	−39.47	68.47†	55.68†
	[−109.61, 6.30]	[60.74, 73.65]	[41.22, 66.54]
RMSE	35.07	8.26†	11.16†
	[21.94, 48.26]	[6.92, 9.94]	[8.73, 16.37]
PME	60.63	24.33†	29.39†
	[21.35, 99.44]	[18.83, 30.04]	[22.95, 44.51]
NME	49.67	8.86†	28.72†
	[15.54, 119.36]	[6.09, 13.36]	[19.98, 37.11]

The test is performed on 100 adult virtual patients of the UVA/Padova simulator. p-values are computed with respect to the average model with the nonparametric Wilcoxon signed-rank test. All the differences are statistically significant with $p < 0.001$. Data are non-normal and are presented in terms of median [25th, 75th] percentiles.
† $p < 0.001$.

A linear approximation of the average nonlinear adult virtual patient has been identified through the presented approaches. The resulting predictions are shown in Fig. 1, where also the subcutaneous glucose of the nonlinear model is depicted. The CO, NP, and the linearized models achieved COD equal to 80.32, 66.14, and 58.97 and FIT equal to 54.96, 41.81, and 32.89, respectively. The CO and the linearized model are characterized by 13 internal states, whereas the NP model includes 121 states.

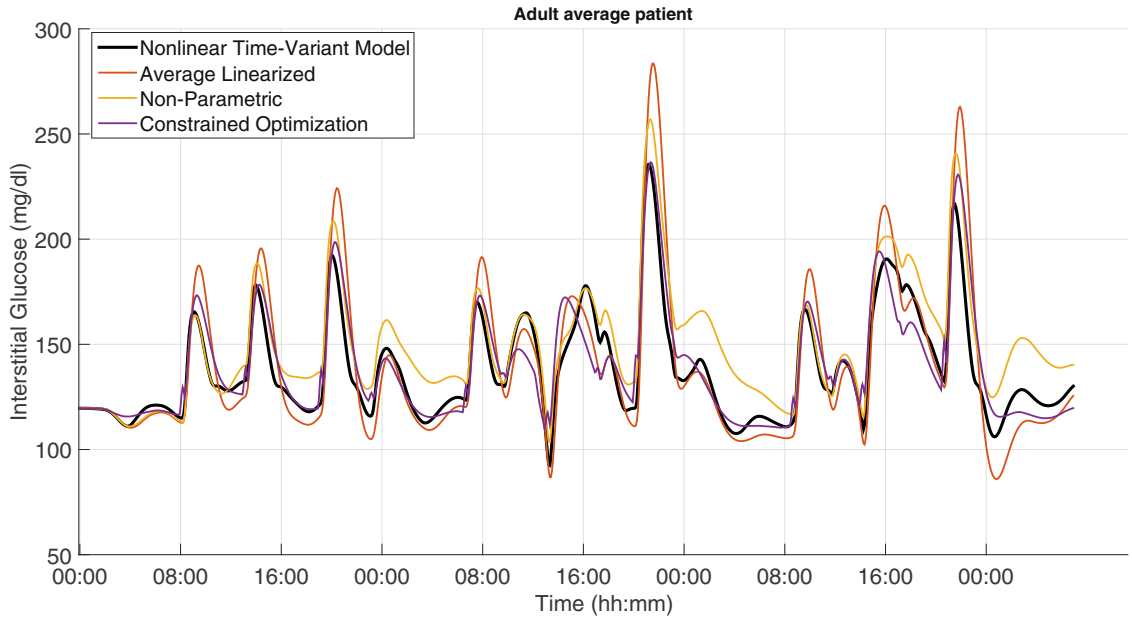

Fig. 1. Validation of the adult average virtual patient. The black line represents the subcutaneous glucose achieved with the nonlinear time-varying model in the test protocol of Table 3. The red, yellow, and violet lines represent the simulations performed with the linearized model and with the identified NP and CO models, respectively. (For interpretation of the references to color in this figure legend, the reader is referred to the web version of this article.)

4. Conclusions

The identified individualized models significantly improve the prediction performance with respect to the linearized average model. The NP models provide the best performance, but are characterized by a non-fixed number of internal states that depend on the chosen realization technique. On the other hand, the postulated parametric structure of the CO models has a fixed number of internal states. While the CO approach does not guarantee the identification of a "valid" model, it requires a shorter identification protocol for parameter estimation that would be more feasible in a real-life scenario. Future works could consider the presented identification approaches for identifying linear models of real patients by relying on pre-filtered data through the retrofit procedure described in Ref. [41], which can substitute the MA filter (14).

The work presented in Ref. [37] demonstrated that MPC based on the NP models are able to significantly improve the closed-loop control performance with respect to a non-individualized MPC. Subsequent works will consider the CO models for in silico closed-loop tests and, in the future, both the presented identification approaches may be proposed for designing individualized controllers for in vivo clinical trials.

References

[1] B.W. Bequette, Challenges and recent progress in the development of a closed-loop artificial pancreas, Annu. Rev. Control 36 (2) (2012) 255–266.
[2] C. Cobelli, C. Dalla Man, G. Sparacino, L. Magni, G. De Nicolao, B.P. Kovatchev, Diabetes: models, signals, and control, IEEE Rev. Biomed. Eng 2 (2009) 54–96.
[3] F.H. El-Khatib, S.J. Russell, D.M. Nathan, R.G. Sutherlin, E.R. Damiano, A bihormonal closed-loop artificial pancreas for type 1 diabetes, Sci. Transl. Med 2 (27) (2010) 27ra27.
[4] R. Hovorka, J.M. Allen, D. Elleri, L.J. Chassin, J. Harris, D. Xing, et al., Manual closed-loop insulin delivery in children and adolescent with type 1 diabetes: a phase 2 randomised crossover trial, Lancet 375 (9716) (2010) 743–751.
[5] S.A. Weinzimer, G.M. Steil, K.L. Swan, J. Dziura, N. Kurtz, W.V. Tamborlane, Fully-automated closed-loop insulin delivery versus semi-automated hybrid control in pediatric patients with type 1 diabetes using an artificial pancreas, Diabetes Care 31 (5) (2008) 934–939.
[6] S.J. Russell, F.H. El-Khatib, M. Sinha, K.L. Magyar, K. McKeon, L.G. Goergen, et al., Outpatient glycemic control with a bionic pancreas in type 1 diabetes, N. Engl. J. Med 371 (2014) 313–325.
[7] S. Del Favero, J. Place, J. Kropff, M. Messori, P. Keith-Hynes, R. Visentin, et al., Multicentre outpatient dinner/overnight reduction of hypoglycemia and increased time of glucose in target with a wearable artificial pancreas using multi-modular model predictive control algorithm in adults with type 1 diabetes, Diabetes Obes. Metab 17 (5) (2015) 468–476.
[8] H. Thabit, A. Lubina-Solomon, M. Stadler, L. Leelarathna, E. Walkinshaw, A. Pernet, et al., Home use of closed-loop insulin delivery for overnight glucose control in adults with type 1 diabetes: a 4-week, multicentre, randomised crossover study, Lancet Diabetes Endocrinol 2 (9) (2014) 701–709.
[9] J. Kropff, S. Del Favero, J. Place, C. Toffanin, R. Visentin, M. Monaro, et al., 2 month evening and night closed-loop glucose control in patients with type 1 diabetes under free-living conditions: a randomised crossover trial, Lancet Diabetes Endocrinol 3 (12) (2015) 939–947. http://dx.doi.org/10.1016/S2213-8587(15)00335-6.
[10] M. Messori, C. Cobelli, L. Magni, Artificial pancreas: from in-silico to in-vivo, in: IFAC 9th International Symposium on Advanced Control of Chemical Processes, 2015, pp. 1301–1309.
[11] B.P. Kovatchev, M.D. Breton, C. Dalla Man, C. Cobelli, In silico preclinical trials: a proof of concept in closed-loop control of type 1 diabetes, J. Diabetes Sci. Technol 3 (1) (2009) 44–55.
[12] C. Dalla Man, F. Micheletto, D. Lv, M. Breton, B. Kovatchev, C. Cobelli, The UVA/PADOVA type 1 diabetes simulator: new features, J. Diabetes Sci. Technol 8 (1) (2014) 26–34.
[13] S. Del Favero, G. Pillonetto, C. Cobelli, G. De Nicolao, A novel nonparametric approach for the identification of the glucose-insulin system in type 1 diabetic patients, in: 18th IFAC World Congress, 2011, pp. 8340–8346.
[14] M. Messori, M. Ellis, C. Cobelli, P.D. Christofides, L. Magni, Improved postprandial glucose control with a customized model predictive controller, in: American Control Conference (ACC), 2015, pp. 5108–5115.
[15] L. Magni, D.M. Raimondo, L. Bossi, C. Dalla Man, G. De Nicolao, B. Kovatchev, et al., Model predictive control of type 1 diabetes: an in silico trial, J. Diabetes Sci. Technol 1 (6) (2007) 804–812.
[16] L. Magni, D.M. Raimondo, C. Dalla Man, G. De Nicolao, B. Kovatchev, C. Cobelli, Model predictive control of glucose concentration in type I diabetic patients: an in silico trial, Biomed. Signal Process. Control 4 (4) (2009) 338–346.
[17] S.D. Patek, L. Magni, E. Dassau, C. Hughes-Karvetski, C. Toffanin, G. De Nicolao, et al., Modular closed-loop control of diabetes, IEEE Trans. Biomed. Eng 59 (11) (2012) 2986–2999.
[18] P. Soru, G. De Nicolao, C. Toffanin, C. Dalla Man, C. Cobelli, L. Magni, MPC based artificial pancreas: strategies for individualization and meal compensation, Annu. Rev. Control 36 (1) (2012) 118–128.
[19] C. Toffanin, M. Messori, F. Di Palma, G. De Nicolao, C. Cobelli, L. Magni, Artificial pancreas: model predictive control designfrom clinical experience, J. Diabetes Sci. Technol 7 (6) (2013) 1470–1483.
[20] M. Messori, E. Fornasiero, C. Toffanin, C. Cobelli, L. Magni, A constrained model predictive controller for an artificial pancreas, in: 19th IFAC World Congress, 2014, pp. 10144–10149.
[21] B.P. Kovatchev, C. Cobelli, E. Renard, S. Anderson, M. Breton, S. Patek, et al., Multinational study of subcutaneous model-predictive closed-loop control in type 1 diabetes mellitus: summary of the results, J. Diabetes Sci. Technol 4 (6) (2010) 1374–1381.

[22] M. Breton, A. Farret, D. Bruttomesso, S. Anderson, L. Magni, S. Patek, et al., Fully integrated artificial pancreas in type 1 diabetes: modular closed-loop glucose control maintains near normoglycemia, Diabetes 61 (9) (2012) 2230–2237.
[23] Y.M. Luijf, J.H. DeVries, K. Zwinderman, L. Leelarathna, M. Nodale, K. Caldwell, et al., Day and night closed-loop control in adults with type 1 diabetes mellitus: a comparison of two closed-loop algorithms driving continuous subcutaneous insulin infusion versus patient self-management, Diabetes Care 36 (12) (2013) 3882–3887.
[24] H.P. Chase, F.J. Doyle III, H. Zisser, E. Renard, R. Nimri, C. Cobelli, et al., Multicenter closed-loop/hybrid meal bolus insulin delivery with type 1 diabetes, Diabetes Technol. Ther 16 (10) (2014) 623–632.
[25] S. Del Favero, D. Bruttomesso, F. Di Palma, G. Lanzola, R. Visentin, A. Filippi, et al., First use of model predictive control in outpatient wearable artificial pancreas, Diabetes Care 37 (5) (2014) 1212–1215.
[26] B.P. Kovatchev, E. Renard, C. Cobelli, H.C. Zisser, P. Keith-Hynes, S.M. Anderson, et al., Safety of outpatient closed-loop control: first randomized crossover trials of a wearable artificial pancreas, Diabetes Care 37 (7) (2014) 1789–1796.
[27] H. Zisser, E. Renard, B. Kovatchev, C. Cobelli, A. Avogaro, R. Nimri, et al., Multicenter closed-loop insulin delivery study points to challenges for keeping blood glucose in a safe range by a control algorithm in adults and adolescents with type 1 diabetes from various sites, Diabetes Technol. Ther 16 (10) (2014) 613–622.
[28] K. Turksoy, A. Cinar, Adaptive control of artificial pancreas systems—a review, J. Healthc. Eng 5 (1) (2014) 1–22.
[29] K. Turksoy, E.S. Bayrak, L. Quinn, E. Littlejohn, A. Cinar, Adaptive multivariable closed-loop control of blood glucose concentration in patients with type 1 diabetes, in: American Control Conference (ACC), 2013, pp. 2905–2910.
[30] K. Turksoy, L. Quinn, E. Littlejohn, A. Cinar, Multivariable adaptive identification and control for artificial pancreas systems, IEEE Trans. Biomed. Eng 61 (3) (2014) 883–891.
[31] C. Toffanin, A. Sandri, M. Messori, C. Cobelli, L. Magni, Automatic adaptation of basal therapy for type 1 diabetic patients: a run-to-run approach, in: 19th IFAC World Congress, 2014, pp. 2070–2075.
[32] C.C. Palerm, H. Zisser, W. Bevier, L. Jovanovic, F.J. Doyle III, Prandial insulin dosing using run-to-run control application of clinical data and medical expertise to define a suitable performance metric, Diabetes Care 30 (5) (2007) 1131–1136.
[33] C.C. Palerm, H. Zisser, L. Jovanovic, F.J. Doyle III, A run-to-run framework for prandial insulin dosing: handling real-life uncertainty, Int. J. Robust Nonlinear Control 17 (13) (2007) 1194–1213.
[34] P. Herrero, P. Pesl, M. Reddy, N. Oliver, P. Georgiou, C. Toumazou, Advanced insulin bolus advisor based on run-to-run control and case-based reasoning, IEEE J. Biomed. Health Inform 19 (3) (2015) 1087–1096.
[35] P. Herrero, P. Pesl, J. Bondia, M. Reddy, N. Oliver, P. Georgiou, et al., Method for automatic adjustment of an insulin bolus calculator: in silico robustness evaluation under intra-day variability, Comput. Methods Programs Biomed 119 (1) (2015) 1–8.
[36] L. Magni, M. Forgione, C. Toffanin, C. Dalla Man, G. De Nicolao, B. Kovatchev, et al., Run-to-run tuning of model predictive control for type I diabetic subjects: an in silico trial, J. Diabetes Sci. Technol 3 (5) (2009) 1091–1098.
[37] M. Messori, C. Toffanin, S. Del Favero, G. De Nicolao, C. Cobelli, L. Magni, A nonparametric approach for model individualization in an artificial pancreas, IFAC-PapersOnLine 48 (20) (2015) 225–230.
[38] G. Pillonetto, G. De Nicolao, A new kernel-based approach for linear system identification, Automatica 46 (1) (2010) 81–93.
[39] G. Pillonetto, A. Chiuso, G. De Nicolao, Prediction error identification of linear systems: a nonparametric Gaussian regression approach, Automatica 47 (2) (2011) 291–305.
[40] S. Kirkpatrick, C.D. Gelatt, M.P. Vecchi, Optimization by simulated annealing, Science 220 (4598) (1983) 671–680.
[41] S. Del Favero, A. Facchinetti, G. Sparacino, C. Cobelli, Improving accuracy and precision of glucose sensor profiles: retrospective fitting by constrained deconvolution, IEEE Trans. Biomed. Eng 61 (4) (2014) 1044–1053.